THE ASTROPHYSICAL JOURNAL, 321:888–897, 1987 October 15

THE RICH MOLECULAR SPECTRUM AND THE RAPID OUTFLOW OF OH 231.8+4.2

MARK MORRIS
Department of Astronomy, University of California, Los Angeles

AND

STÉPHANE GUILLOTEAU, ROBERT LUCAS, AND ALAIN OMONT
Groupe d'Astrophysique,[1] Observatoire de Grenoble, Université Scientifique Technologique et Médicale de Grenoble
Received 1987 January 15; accepted 1987 April 6

ABSTRACT

Emission lines of eight molecules were observed in the circumstellar outflow of the bipolar nebula OH 231.8+4.2. Five of these molecules, including HNC, CS, and NH_3, were previously undetected in this object, and two of these—HCO^+ and OCS—are reported for the first time in any post–main-sequence circumstellar outflow. The relatively large abundance of HCO^+ ($\sim 10^{-7}$) is attributable to the presence of an internal source of ionization. Thermal SiO emission was observed, implying that condensation of this molecule onto grains is somehow inhibited or that it is subsequently removed from the grains. Of the 13 molecules now known in this outflow (far more than in any other oxygen-rich envelope), five contain sulfur. The total abundance of sulfur-containing molecules, dominated by SO_2, implies that almost all sulfur is accounted for if the mass-loss rate is $\sim 10^{-4}\ M_\odot\ yr^{-1}$. A discussion of the circumstellar chemistry in OH 231.8+4.2 is presented; ion molecule reactions can account for the observed HCN, HNC, and CS—molecules that are not expected to have observable abundances in an oxygen-rich environment. Shocks may be important for producing the sulfur molecules with their observed abundances.

The line profiles indicate that the emission arises in two kinematic components. One gives rise to roughly triangular profiles which are 80 km s^{-1} wide at the base and dominates the emission from most molecules. The other gives rise to broad, flat profiles up to 200 km s^{-1} in total extent. A brief map of CO $J = 1$–0 emission reveals that the narrower component is unresolved with 21″ resolution, whereas the blue and red wings of the broad component are extended along the polar axis, to the north and the south, respectively. When the tilt of this axis is taken into account, one finds that the outflow velocity of the polar molecular jets is greater than 140 km s^{-1}. An examination of the latitude dependence of the outflow velocity and mass-loss rate is presented.

Subject headings: interstellar: molecules — nebulae: abundances — nebulae: individual (OH231.8+4.2)

I. INTRODUCTION

The remarkable bipolar nebula OH 231.8+4.2, or OH 0739−14 (the Rotten Egg Nebula), is unusual in several respects:

1. *Kinematically*, it stands out among OH/IR stars in having the largest known outflow velocity—30–300 km s^{-1}, apparently depending on the angle with respect to the system's polar axis (i.e., the axis of symmetry joining the two reflection nebulae). The full width of the unusually flat OH maser profile is 100 km s^{-1} (Turner 1971; Morris and Bowers 1980), and the full width of the CO line approaches 200 km s^{-1} (this paper). Furthermore, the object appears to have an associated jet of Hα-emitting gas which streams along its polar axis at velocities up to 100 km s^{-1} (Cohen *et al.* 1985, hereafter referred to as CDST).

2. *Chemically*, it appears oxygen-rich by virtue of its OH, H_2O, and SiO masers (Morris and Knapp 1976; Bowers and Morris 1984; Barvainis and Clemens 1984) and its remarkably strong lines of the sulfur-containing molecules H_2S, SO_2, and SO (Ukita and Morris 1983; Guilloteau *et al.* 1986). But, in addition, it displays emission from HCN, which, under equilibrium conditions, is normally considered an indicator of a carbon-rich circumstellar chemistry (Deguchi and Goldsmith 1985; Deguchi, Claussen, and Goldsmith 1986).

3. *Thermally*, it has a very cool dust envelope (Kleinmann *et al.* 1978; Sopka *et al.* 1985), which helps account for its uncommon characteristic of having both gaseous and solid H_2O in its envelope (Soifer *et al.* 1981; Jura and Morris 1985).

4. *Morphologically*, it is a rather narrow bipolar nebula in the near-infrared continuum, and each of the bipolar lobes is accompanied by knots resembling Herbig-Haro objects, presumably at the position where the bipolar jets undergo shocks as they encounter slower moving material (CDST). Even at wavelengths as long as 3.5 μm, the object is unusually extended for a circumstellar outflow from an evolved star because of reflection by dust (Allen *et al.* 1980; Dyck *et al.* 1984; Tielens, Werner, and Capps 1985). An Hα image recently made by Reipurth (1987) shows that the bipolar lobes are ionized by an internal source, that the ionization front is ionization bounded at about the positions of the HH objects, and that the lobes are asymmetric, with the southern ionized region being larger than the one to the north. This asymmetry is similar to the brightness asymmetry of the two near-infrared reflection nebulae. The geometry of the OH maser is rather striking: the knots of emission have a clear symmetry about the system's polar axis and are extended along that axis, a circumstance which is unique among known stellar masers (Morris, Bowers, and Turner 1982).

Because OH 231.8+4.2 (hereafter OH 231.8) has so many prominent and unparalleled characteristics, it may provide

[1] U.A. 708 du CNRS.

important clues to the nature of the mass ejection mechanism in at least one class of cool, mass-losing objects. For example, the suggestion that the mass loss in bipolar nebulae is affected by, if not caused by, the presence of a close binary companion to the red giant primary (Morris 1981) has been supported by the observation by CDST (see also Cohen 1985) of an enhanced blue continuum in OH 231.8, which they suggest might imply the presence of a hot companion to the M9 III primary (Cohen 1981). We have therefore undertaken to study this object in molecular line emission, hoping to shed further light on its chemistry, its structure, and its evolution. The radio observations of a number of molecules, including the first observations in any circumstellar envelope of HCO^+ (or any molecular ion) and OCS, are reported in § II. The results of an earlier observation of SO_2 and SO reported by some of us elsewhere (Guilloteau *et al.* 1986) are included for completeness. The implications of these data for the structure and composition of OH 231.8 are discussed in § III and IV, respectively. In § V, the implications of the HCO^+ detection are discussed, and in § VI, the many observed sulfur compounds are considered with regard to circumstellar chemical processes which may account for their high abundance.

II. OBSERVATIONS

The millimeter observations were made in 1986 March with the IRAM 30 m telescope. The beam size is 27″ at 90 GHz and 21″ at 111 GHz, and aperture and beam efficiencies are 0.53 and 0.60 at 90 GHz, and 0.49 and 0.56 at 111 GHz, respectively. The pointing accuracy over the whole sky was about 5″ rms, but better pointing was achieved by frequent monitoring of continuum sources close to OH 231.8. Tracking accuracy is better than 1″ rms. We used a Schottky diode mixer above 95 GHz, and an SIS junction mixer below. The total SSB system temperatures referred to above the atmosphere, and corrected for antenna losses, were typically 700 K and 1600 K for the two receivers, respectively.

Baseline quality of both receivers proved good. All spectra were obtained with the 512 × 1 MHz filter bank spectrometer, split into two 256 channel halves, to enable observation of two lines simultaneously (one with each receiver). The 100 kHz filters were usually centered on the SiO ($V = 1$) line to provide a check on the pointing and source velocity. Linear baselines have been removed from all spectra. All results are given in terms of main beam brightness temperature (T_A^*). The main source of uncertainty in T_A^* is the image sideband gain ratio (up to a factor of 2). Observations of HCO^+, HCN, and HNC were rescaled by observing Orion A as a line calibrator (calibrated spectra of this source obtained with a single sideband Fabry-Perot filter are available at these frequencies).

The NH_3 observations were made on 1986 July 26–27 with the Effelsberg 100 m telescope. The receiver was a maser amplifier which gave a total system temperature referred to above the atmosphere, and corrected for antenna losses, of about 500 K. The backend was an autocorrelator split in two banks of 512 channels and 50 MHz bandwidth centered on the (1, 1) and (2, 2) lines, respectively (resolution 2.88 km s^{-1}). The beam size is near 42″. Pointing was checked every hour and the accuracy was 3″ rms. Third-order polynomial baselines were removed from the spectra, but the lines were clearly visible without any baseline removal.

The measurements from both telescopes are listed in Table 1. Column (4) lists T_A^* corrected for atmospheric absorption and for beam efficiency and beam coupling factors. The integral of this quantity over the entire line profile is given in column (5), the central velocity is listed in column (6), and the full line width at half-maximum intensity is presented in column (7). (The full line width at zero intensity is not reported because of the nonstandard profile; the weak, broad wings

TABLE 1

OBSERVATIONAL RESULTS

Molecule (1)	Line (2)	Frequency (MHz) (3)	T_A^* (peak) (K) (4)	A[a] (K km s^{-1}) (5)	V[a] (km s^{-1}) (6)	ΔV[b] (km s^{-1}) (7)
^{12}CO	1–0	115271.2	1.30	92.5 ± 4.2	29.7 ± 1.1	111 ± 4
					33.6 ± 0.4	31 ± 2[c]
^{13}CO	1–0	110201.4	0.45	21.3 ± 0.7	30.0 ± 0.7	45 ± 2
$H^{12}CN$	1–0	88631.6	0.65	30.0 ± 1.0	30.4 ± 0.6	41 ± 2
$H^{13}CN$[d]	1–0	86339.9	0.11	3.5 ± 0.4	31.3 ± 1.8	31 ± 4
HNC	1–0	90663.6	0.27	12.0 ± 0.9	27.5 ± 1.0	32 ± 4
CS	2–1	97981.0	0.26	11.7 ± 0.5	30.0 ± 0.8	42 ± 2
HCO^+	1–0	89188.6	0.10	18.1 ± 0.9	18.2 ± 4.1	190 ± 14[c]
SiO	2–1	86846.9	0.09	7.5 ± 0.5	27.1 ± 2.8	76 ± 6
OCS	8–7	97301.2	0.09	3.6 ± 0.5	42.6 ± 2.8	39 ± 6
SO_2[d]	3_{13}–02_2	104029.4	1.28	61.4 ± 1.1	36.3 ± 0.4	45 ± 1
SO[d]	2_2–1_1	86093.9	0.20	7.1 ± 0.5	33.0 ± 1.2	33 ± 3
CN	1, 3/2–0, 1/2	113491.0	<0.15	<3.4	...	...
HC_3N	10–9	90979.0	<0.08	<1.6	...	...
SiS	5–4	90771.5	<0.09	<1.8	...	...
N_2H^+	1–0	93174.0	<0.06	<1.2	...	...
HCS^+	2–1	85347.9	<0.13	<2.5	...	...
NH_3	(1, 1)	23694.5	0.09	4.9 ± 0.5	28.5 ± 2.5	51 ± 6
NH_3	(2, 2)	23722.6	0.05	2.4 ± 0.4	44.7 ± 3.4	41 ± 6[e]

[a] Integrated intensity (A) and velocity (V) obtained from Gaussian fit to profile.
[b] Full line width at half-maximum.
[c] Results of a two-component Gaussian fitting.
[d] Result from Guilloteau *et al.* 1986 reproduced for completeness.
[e] Unreliable because of baseline curvature.

render this quantity ambiguous.) Figure 1 shows the profiles of all of the detected transitions from both telescopes. Note that the full extent of the emission approaches 200 km s^{-1} in the ^{12}CO profile (consistent with the noisier spectrum published previously by Knapp and Morris 1985), but, with the exception of HCO^+ and SiO, the emission in most profiles is confined to the LSR velocity range -10 to $+70$ km s^{-1}. A measurement of the ^{13}CO profile in OH 231.8 was reported earlier by Knapp and Chang (1985). Their integrated $^{12}CO/^{13}CO$ intensity ratio, 5.6 ± 1.5, is in agreement with our measurement: 4.36 ± 0.25.

A map of ^{12}CO emission in the $J = 1 \rightarrow 0$ line was made with the 30 m IRAM telescope. The spectra, which were taken at 10″ intervals on a NSEW grid, are shown in Figure 2. The apparent offset of the position of peak emission to the east may be due to a pointing error of 3″ or 4″. It was not reproducible on subsequent east-west scans and is therefore not a reliable result. The north-south extension was not only reproducible but is clearly velocity-dependent, indicating that we have resolved some of the source structure in this direction. The implications of this will be discussed below.

The OH maser and the near-infrared continuum of

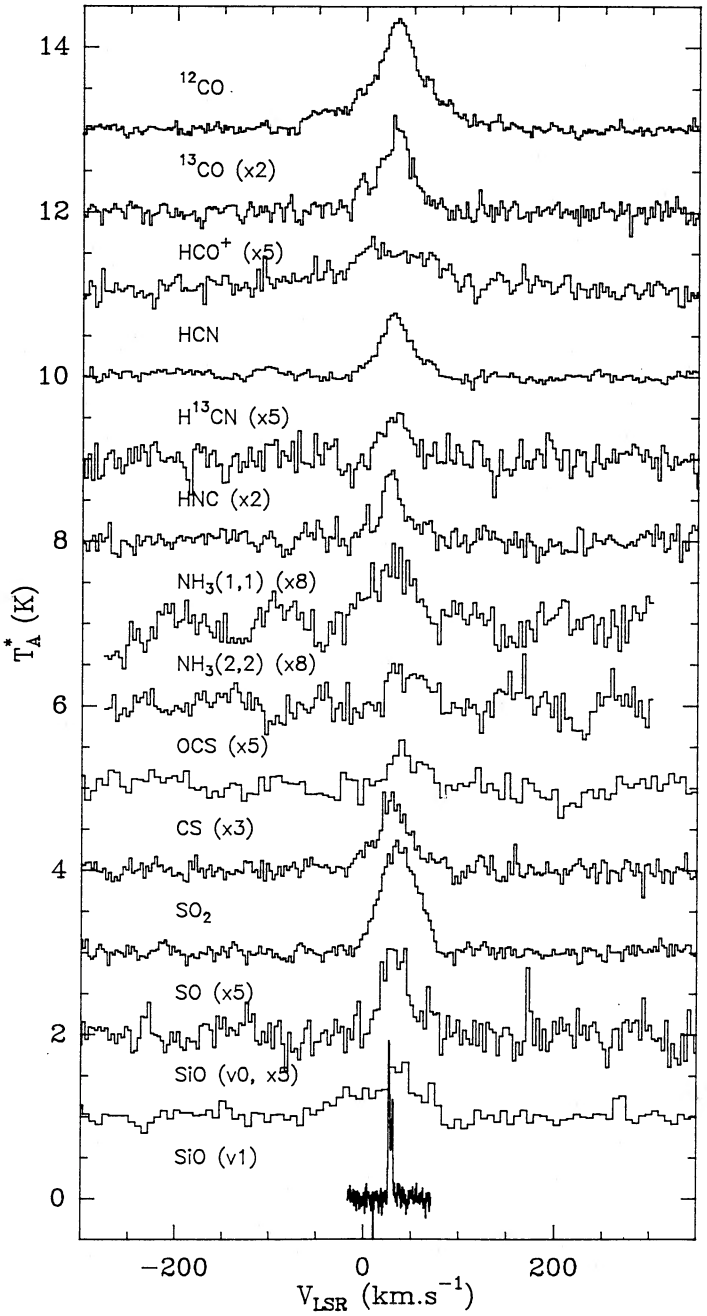

FIG. 1.—Spectra of the molecular lines detected in OH 231.8 + 4.2. The number following the molecule name is the scaling factor of the spectrum. Units are main beam brightness temperatures.

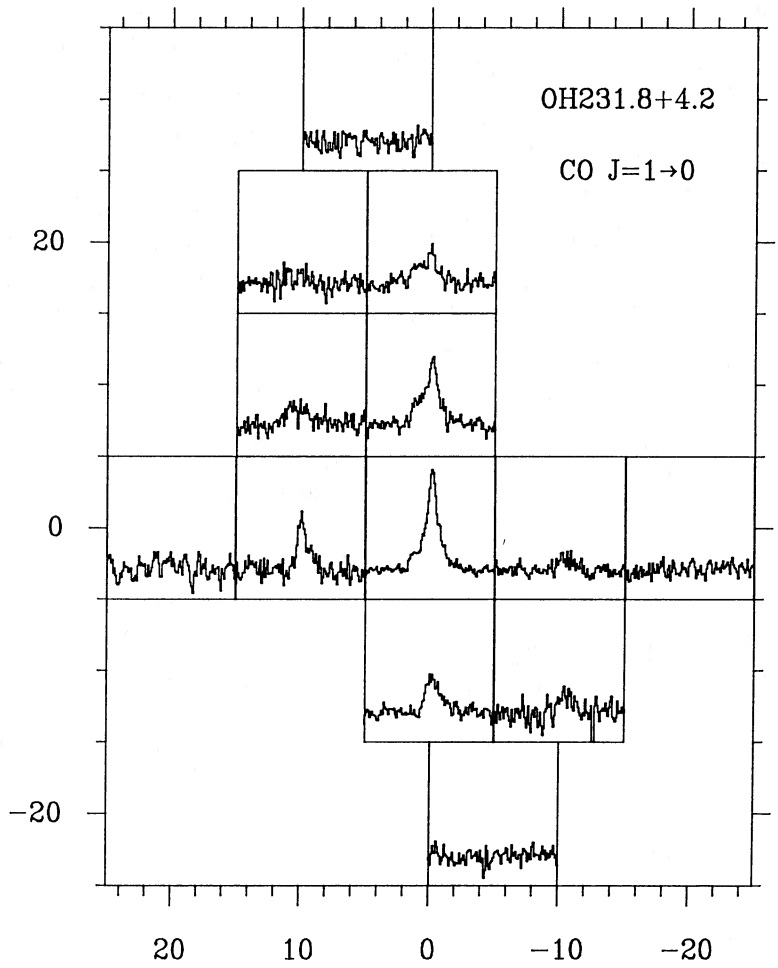

FIG. 2.—Map of the CO $J = 1$–0 line emission towards OH 231.8+4.2. The velocity scale of each spectrum is -250 to 300 km s^{-1} and the temperature scale -0.4 to 1.5 K main beam brightness temperature. The coordinates are offsets in arcseconds in right ascension and declination with respect to the source position, $\alpha = 7^h39^m59^s.0$, $\delta = -14°35'41''$ (1950.0). The beam size is $\sim 21''$.

OH 231.8+4.2 vary strongly during the $\sim$684 day period of the star (Feast *et al.* 1983; Bowers and Morris 1984). It is possible that some of the lines we have observed vary in response. We note, however, that most of our spectra were taken near maximum light. With the exception of SO, SO_2, and NH_3, the observations took place only $\sim$5 weeks after the near-infrared observations of Reipurth (1987), which, he argues, were at or near maximum light.

III. THE KINEMATICAL STRUCTURE OF THE ENVELOPE

The profile of the ^{12}CO line can be decomposed into two components centered at about the same LSR velocity, $\sim$30 km s^{-1}, as indicated in Table 1. The first is a roughly triangular component having a total width at zero power of $\sim$75 km s^{-1}. This component is the only one present in most of the line profiles and is best illustrated by the SO_2 profile. The other component is much broader (total width $\sim$150–200 km s^{-1}) and flatter and is the dominant component in the HCO^+ and SiO profiles.

In the CO map, the two components of the profile behave differently: the central, triangular component is probably unresolved, while the broad component is extended along the polar axis, with the blue wing extended to the north, and the red wing predominant in the spectrum taken immediately to the south of the central position. The broad component therefore suggests a biconical outflow in which the highest velocity gas flows out along the polar axis. This picture is consistent with that of CDST, who find blue(red)-shifted Hα emission along the northern (southern) polar axis. The radial velocities of the high-velocity CO and Hα emission, relative to the star, are comparable ($\pm$73 km s^{-1} for Hα vs. $\pm$100 km s^{-1} for the most extreme CO emission). Following CDST, we correct for an inclination of 47° and arrive at the remarkable conclusion that CO is flowing in both directions along the polar axis at greater than 140 km s^{-1}.

The velocity measurements of CDST, verified by those in this paper, coupled with the phase lag measurements of Bowers and Morris (1984), indicate unambiguously that the dim northern lobe is the nearer one. This contrasts with the OH maser model of Morris, Bowers, and Turner (1982), who assumed complete symmetry about the equatorial plane in order to deduce that the dimmer lobe is the more distant one on the basis of the presumption that it is subject to extinction by dust near the equatorial plane. That model must be discarded, since there is a real asymmetry between the brightness of the lobes. One must conclude that the OH masers arise at relatively high latitudes near the polar axis. The spatial extent and the velocity field of the OH emission therefore agree quite well with those

of CO, except that the extreme CO velocities exceed the extreme OH maser velocities by a factor of 2.

The asymmetry of the envelope about the equatorial plane is evident in the OH maser data (Bowers and Morris 1984) and in the data of this paper as well: the high-velocity emission in those molecular line profiles that display it is more prominent on the blue side, corresponding to the northern lobe. This effect is most pronounced in the thermal SiO profile; there, the blue wing is quite prominent while the red wing is simply absent. Also, the spatial extent of the high-velocity CO emission appears to be greater to the north than to the south (Fig. 2). Finally, the Hα emission is quite asymmetric (Reipurth 1987), showing a much greater extent to the south than to the north. Two alternative explanations for the asymmetry arise: (1) the mass-loss rate is greater to the north than to the south, or (2) the rate of ionization, caused by an internal source of ionization, is greater to the south, and therefore a greater portion of the mass lost in that direction is ionized. In either case, the asymmetry is internally generated—a curious circumstance which is not readily explicable.

The central triangular part of the line profiles is unusual for a circumstellar outflow; most molecular outflows from evolved objects display flattened or rounded profiles with steep sides (Morris 1985). The differentiating characteristic of OH 231.8 is probably tied to its axisymmetry: it has been suggested (Ukita and Morris 1983) that the outflow velocity may depend on latitude (measured with respect to the polar axis). The presence of the high-velocity polar flow is consistent with that suggestion.

In an attempt to constrain the velocity law that may govern this envelope, we have constructed line profiles for optically thin emission from model envelopes. Both the outflow velocity, v, and the mass-loss rate, $\dot{M}$, were assumed to be functions only of latitude, θ. Many empirical forms were tried, including, for example,

$$v(\theta) = A(B + \sin^n \theta) ,$$
$$\dot{M}(\theta) = \begin{cases} C , & |\theta| > \theta_{\rm crit} , \\ C(\theta/\theta_{\rm crit})^m , & |\theta| < \theta_{\rm crit} . \end{cases} \quad (1)$$

The scaling factors A and C do not affect the profile shapes, so in this particular model, there are a total of five adjustable parameters: B, n, $\theta_{\rm crit}$, m, and i, the inclination of the polar axis with respect to the line of sight. The excitation temperature is assumed to be constant, and, according to the equation of continuity, the density at any point (r, θ) is proportional to $\dot{M}(\theta)/v(\theta)$, so we have weighted the contribution to the intensity from each point by that quantity. We furthermore assume that the radial extent of the emitting region varies linearly with v, and that there are no effects due to the finite resolution of the telescope. (Indeed, the former assumption is consistent with the fact that we do observe the highest velocity regions to be the most extended in ^{12}CO emission.)

Finally, in our modeling, we are guided by the appearance of the bipolar nebula (CDST; Reipurth 1987). It appears quite unlikely that i is small; otherwise, the bipolar lobes should overlap. We have therefore concentrated our investigation to $i > 30°$. This is consistent with $i = 47°$, suggested by CDST.

Two conclusions were drawn from the profile-fitting exercise.

1. In order to avoid steep-sided profiles and negligible emission at high velocities, the amount of mass in the high-velocity, high-latitude flow must not be much smaller than that in the low-velocity, low-latitude flow. This can be seen directly from the ^{12}CO profile, in which the area of the high-velocity component of the emission is similar to that in the central, triangular part of the profile. Of course, the ^{12}CO line probably has a large opacity near line center (see below), so this analysis should be applied to a low-noise profile of an optically thin line such as that of ^{13}CO. Unfortunately, the high-velocity wings of our present ^{13}CO profile are buried in the noise. Taking account of opacity will reduce the derived high-velocity mass relative to low-velocity mass, but one should also keep in mind that the total solid angle at low latitudes exceeds that at high latitudes, so that the mass-loss rate per unit solid angle could be roughly constant. The definition of "high velocity" or "high latitude" is imprecise since the function $v(\theta)$ is not determined. This conclusion is strengthened if we consider the variation of relative abundance with latitude that may be caused by UV or shock dissociation, since these would predominate at high latitudes.

2. It is possible to reproduce the profiles without any mass loss near the equatorial plane. In fact, when a mass outflow near the equatorial plane having an outflow velocity exceeding a few km s^{-1} is included in the models, it is difficult to produce a centrally peaked profile unless the mass-loss rate in that portion of the outflow is strongly diminished relative to that at high latitudes. For example, the character of the profiles (roughly triangular profiles with substantial wings extending to high velocities) can be reproduced with the following parameters in the empirical model given above: $B = 0$, $n = 3$, $m = 2$, $\theta_{\rm crit} = 30°$, and $i = 65°$.

We cannot rule out mass loss in the equatorial plane, but the possibility that it is absent must be seriously considered. Millimeter interferometer observations will be invaluable for deciding this issue. The implications for the mass-loss mechanism are profound. The binary ejection mechanism suggested by Morris (1981) for bipolar nebulae predicts that the mass loss should be a maximum in the equatorial plane. If it is not, and if OH 231.8 is a binary system, it would appear that an equatorial disk—presumably a rotating accretion disk—is playing a major role in directing, if not originating, the outflow.

IV. MOLECULAR ABUNDANCES

a) Procedures and Assumptions

In contrast to many circumstellar envelopes, the line profiles from OH 231.8 do not provide much information about optical depths because of the strong deviations of the envelope from spherical symmetry. We therefore proceed by initially assuming that all of the observed molecular transitions are optically thin. The deviations from spherical symmetry then do not affect the derivation of abundances because, regardless of the geometry, the area under the line profile is proportional to the total number of molecules. We therefore refer the calculation to the spherically symmetric case. Then, the antenna temperature (constant across the profile in the spherically symmetric case), measured by an ideal, lossless antenna with a Gaussian beam of full width at half-maximum equal to B is

$$T_a^\dagger = \frac{8 \ln 2}{B^2 D^2} \int_0^{p_{\rm max}} p T_B(p) \exp\left(-4 \ln 2 \frac{p^2}{B^2 D^2}\right) dp , \quad (2)$$

where D is the distance to the source, p is the projected distance from the central star, and $p_{\rm max}$ is the outermost radial extent of

the emitting region. The brightness temperature at p is given by

$$T_B(p) = \frac{2\pi^2\mu_0^2}{3k}\frac{vf\dot{N}S}{v^2}\frac{n_u(p)}{p} \quad (3)$$

(cf. Ukita and Morris 1983), where μ_0 is the molecule's permanent dipole moment, and f its fractional abundance by number with respect to H_2. S and v are the line strength and frequency of the transition, and n_u is the fractional sublevel population of the upper state. The symbol k is Boltzmann's constant, and $\dot{N}$ is the total loss rate of molecules per second, which we assume to be dominated entirely by H_2.

We now make the simplifying assumption that the excitation temperature, T_{ex}, is constant throughout the envelope. Although this assumption is a hoax, it often turns out to describe the envelope-averaged level populations surprisingly well (Olofsson *et al.* 1982). Then n_u can be expressed in terms of T_{ex}, and equation (2) becomes, using equation (3),

$$T_a^\dagger = 2\times 10^{13}\frac{\dot{M}(M_\odot\ \mathrm{yr}^{-1})}{v^2(\mathrm{km\ s^{-1}})D(\mathrm{pc})}\frac{f\mu_0^2(\mathrm{debye})}{Z(T_{ex})} \times \frac{\nu(\mathrm{MHz})S\ \exp\left[-1.44E_u(\mathrm{cm}^{-1})/T_{ex}\right]}{B(\mathrm{arcsec})} \times \int_0^{2(\ln 2)^{1/2}p_{\max}/(BD)} \exp(-x^2)dx\ . \quad (4)$$

Here $Z(T_{ex})$ is the molecular partition function, and E_u is the energy of the upper state of the transition. Finally, for a spherical envelope, equation (4) can be inverted to give f by equating $T_a^\dagger$ to the measured temperature, T_A^*.

For the case of OH 231.8, the procedure is somewhat more complicated because the outflow velocity, v, is not well defined. We therefore attempt to confine the abundance analysis to the kinematical component responsible for most of the emission, the so-called triangular component. Since this component lies between -10 and $+70$ km s^{-1}, we define the mean outflow velocity to be 30 km s^{-1} and equate the observed antenna temperature integrated over this velocity range to $2T_A^\dagger v$. The excitation temperature for molecules in OH 231.8 was taken to be 25 K, the rotational temperature determined by Guilloteau *et al.* (1986) from the measured ratio of two SO_2 lines. The intensity ratio of the NH_3 (1, 1) and (2, 2) lines gives a rotational temperature (27 ± 4 K) which is consistent with the assumed 25 K.

The distance to OH 231.8 appears to be a reasonably well-determined quantity now that the geometry of the OH maser is understood. From their phase lag and VLA measurements, Bowers and Morris (1984) found $D = 1300$ tan (i') pc, where i' is the angle between the line of sight and the line joining the extreme high- and low-velocity OH-emitting regions. Now that we are led to identify this line with the polar axis ($i = i'$), we can use the CDST value of 47° for i to arrive at $D = 1300$ pc.

The mass-loss rate is more uncertain: Knapp and Morris (1985) find $10^{-4}\ M_\odot$ yr^{-1} assuming normal abundances, but Jura and Morris (1985) open the possibility of a hydrogen deficiency in this object, in which case $\dot{M}$ could be as small as $10^{-5}\ M_\odot$ yr^{-1}. We adopt $10^{-4}\ M_\odot$ yr^{-1}, noting that all abundances scale inversely with $\dot{M}$.

b) Results

The molecular abundances derived for OH 231.8 are presented in Table 2. This table also lists all the molecular parameters used in the calculation. The absolute abundances depend on the uncertain mass-loss rate, but the relative abundances between molecules should be accurate, except for those molecules whose measured lines are probably optically thick, such as ^{12}CO and $H^{12}CN$ (discussed below). Also, those profiles which display the very broad emission feature may have their triangular component contaminated by high-velocity emission

TABLE 2

MOLECULAR ABUNDANCES

Molecule	Line	S	μ (D)	E_u (cm^{-1})	Z[a]	A[b] (K km s^{-1})	f[c]
^{12}CO	$1\rightarrow 0$	1	0.112	3.845	9.04	66.5	2.8×10^{-4}
^{13}CO	$1\rightarrow 0$	1	0.112	3.676	9.45	20.7	1.0×10^{-4}
$H^{12}CN$	$1\rightarrow 0$	1	2.984	2.956	11.75	29.8	3.9×10^{-7}
$H^{13}CN$	$1\rightarrow 0$	1	2.984	2.880	12.07	3.4	4.8×10^{-8}
HNC	$1\rightarrow 0$	1	2.9	3.024	11.96	13.4	1.8×10^{-7}
CS	$2\rightarrow 1$	2	1.958	4.902	21.26	11.4	2.8×10^{-7}
HCO^+	$1\rightarrow 0$	1	3.3	2.975	11.68	7.9	8.4×10^{-8}
SiO	$2\rightarrow 1$	2	3.098	4.345	24.0	5.6	7.8×10^{-8}
OCS	$8\rightarrow 7$	8	0.715	14.605	85.6	3.3	1.1×10^{-6}
SO_2	$3_{13}\rightarrow 2_{02}$	2.02	1.633	5.382	141.8	58.7	1.3×10^{-5}
SO	$2_2\rightarrow 1_1$	1.5	1.55	13.424	55	7.3	2.1×10^{-6}
NH_3	(1, 1)	1.5	1.468	16.24	3.55	4.6	1.0×10^{-6}
H_2S[d]	$1_{10}\rightarrow 1_{01}$	1.5	0.974	19.376	6.67	3.0	7.5×10^{-7}
CN	$1, 3/2\rightarrow 0, 1/2$	1	1.45	3.786	13.78	<5.1	$<2.0\times 10^{-7}$
HC_3N	$10\rightarrow 9$	10	3.724	16.69	114.5	<2.4	$<4.1\times 10^{-8}$
SiS	$5\rightarrow 4$	5	1.73	9.11	57.4	<2.7	$<1.4\times 10^{-7}$
N_2H^+	$1\rightarrow 0$	1	2.4	3.108	11.2	<1.8	$<1.6\times 10^{-8}$
HCS^+	$2\rightarrow 1$	2	1.86	2.847	24.4	<3.6	$<1.5\times 10^{-7}$

[a] Z is the partition function for an assumed global rotational temperature of 25 K. For linear molecules, $Z = kT_{rot}/B$. Values for Z for SO_2 and SO are taken from Guilloteau *et al.* 1986.

[b] A is the area integrated over the velocity range -10 to 70 km s^{-1}.

[c] f is the fractional abundance by number for an H_2 mass-loss rate $\dot{M}$ of $10^{-4}\ M_\odot$ yr^{-1}.

[d] H_2S data from Ukita and Morris 1983.

which falls within the -10 to $+70$ km s^{-1} range because of projection effects. Thus, the abundances given for HCO^+ and SiO may exceed the actual abundance in the region responsible for the triangular component, and they should therefore be regarded as upper limits for this component.

c) CO, HCN *and the* $^{12}C/^{13}C$ *Ratio*

The emission from ^{12}CO falls into the optically thick regime as defined by Knapp and Morris (1985): $f^{0.85}\dot{M}$ ($M_\odot$ yr^{-1})/v(km s^{-1})$^2 > \sim 5 \times 10^{-12}$. This inequality holds for all velocities in the line profile. Therefore, the value of f derived for this molecule using the optically thin assumption is much too small. By the same argument, ^{13}CO also appears to have optically thick emission, at least in the region responsible for the triangular component of the line profile. When we crudely take the line opacity into account by applying radiative transfer calculations tailored for a spherically symmetric envelope (e.g., Morris, Lucas, and Omont 1984) to the triangular component of the profile (thus jamming a round peg into a triangular hole), we find $f(^{12}CO) = 2 \times 10^{-4}$ and $f(^{13}CO) = 5 \times 10^{-5}$, assuming $\dot{M} = 10^{-4}\ M_\odot$ yr^{-1}.

Emission from HCN is probably also optically thick. The same spherically symmetric radiative transfer calculation gives $f(H^{12}CN) = 6 \times 10^{-7}$ and $f(H^{13}CN) = 5 \times 10^{-8}$. These numbers suggest that the isotope ratio is quite small in the source (~ 10), but this result is not very reliable. A lower limit to the isotope ratio is obtained from the line intensity ratios at the highest velocities in the profiles where the line opacity is minimized. (Note that this contrasts with the spherically symmetric case, where the line opacity is maximized in the wings.) In the CO profiles, the maximum significant line ratio is greater than ~ 8, comparable to that of HCN. Of course, when line ratios are compared over a range of a few hundred km s^{-1}, one must be especially attentive to the possibility of baseline fluctuations; the numbers quoted here are probably not corrupted by baseline effects.

We conclude that the $[^{12}C]/[^{13}C]$ ratio is probably smaller than the solar system value, but that more sensitive measurements of the rarer isotopic species are needed in order to get a well-determined value. Given the enhancement of nitrogen in this object (CDST), it would not be surprising if CNO-processing has also lowered the $[^{12}C]/[^{13}C]$ ratio.

a) N-*rich Molecules*

i) NH_3

Ammonia is the most abundant of the observed N-containing molecules (the quasi totality of nitrogen should be in the form of N_2). Its abundance ($>10^{-6}$) is more than two orders of magnitude larger than foreseen by thermodynamical equilibrium at 1000 K in the atmosphere of a giant star of solar composition (Tsuji 1973), and it is one order of magnitude larger than the NH_3 abundance inferred for the outflow from the carbon star IRC +10216 (Betz and McLaren 1980). The observed abundance implies either that thermodynamical equilibrium is achieved well below 1000 K, even with the large overabundance of N reported by CDST; or, more probably, that there exists some internal source of free N atoms (UV, shocks, etc); in the warm inner layers, atomic N is readily converted into NH_3 by successive reactions with H_2 if the H/H_2 ratio does not exceed a few percent (Slavsky and Scalo 1986). Ionic reactions are probably less efficient in producing NH_3, because of the same difficulties as encountered in the discussion of the formation of interstellar ammonia (see, e.g., Langer 1985).

ii) The Formation of HCN

Thermodynamical equilibrium at $T \approx 1000$ K would yield a ratio $NH_3/HCN \approx 10^2$ (Tsuji 1964). Accordingly, the observed abundance of HCN ($\sim 4 \times 10^{-7}$) would be even more difficult to account for with this hypothesis than the rather high NH_3 abundance. The presence of such a large amount of HCN implies some nonequilibrium processes which remove both C and N from their main reservoirs. For N, the task can be alleviated by the existence of a large abundance of NH_3, which is less stable than N_2. The main problem is then the dissociation of CO, which can occur by photodissociation or by shocks.

Photodissociation of both CO and N_2 by galactic UV, followed by neutral radical reactions has been suggested by Deguchi, Claussen, and Goldsmith (1986). However, the predicted abundance of HCN falls more than an order of magnitude short of that observed, even though their abundance of neutral C is probably largely overestimated.

A more promising route is the reaction of C^+, photoproduced from CO, with NH_3:

$$C^+ + NH_3 \rightarrow HCNH^+ + H\ , \qquad (5)$$

followed by dissociative recombination of $HCNH^+$ giving HCN or HNC (see below). With the fast rate of equation (5), a large fraction of NH_3 will be converted to HCN if $n(C^+) > 10^{-2}$ cm^{-3} at $r \approx 10^{17}$ cm. This is the same order of magnitude of C^+ predicted by the model of Mamon, Glassgold, and Omont (1986), which assumes only an external source of UV radiation. Although the results could be relatively sensitive to the details of the photodissociation of C^+ and NH_3, the amount of HCN produced would probably be even greater if an internal source of UV radiation is added.

Another route could be

$$\begin{aligned} C^+ + H_2 &\rightarrow CH_2^+ + h\nu\ , \\ CH_2^+ + H_2 &\rightarrow CH_3^+ + H\ , \\ CH_3^+ + N &\rightarrow HCNH^+ + H\ . \end{aligned} \qquad (6)$$

However, this sequence is probably far less effective than reactions (5) because most of the CH_3^+ produced should be destroyed by reactions with e^- or O.

An alternative possibility is that atomic C (and N) are produced by dissociative shocks, i.e., those in which $v > 20$ km s^{-1} (Hollenbach and McKee 1980; Mitchell 1984). Although detailed models could be extremely difficult to construct, the formation of HCN could then be easily achieved in subsequent nondissociative shocks (Mitchell 1984), or by ion chemistry (eq. [5], etc.) in the external layers.

iii) The HNC/HCN Ratio

The HNC line is unusually strong in OH 231.8. Its integrated intensity is about half that of the HCN line, which contrasts with the carbon-rich object IRC +10216, in which the intensity ratio is about 1/8 (Johansson *et al.* 1984). The HNC line is narrower than the HCN line, presumably because it has a smaller opacity, although we cannot rule out the possibility that the two molecules have different distributions. Under the optically thin assumption, the abundance ratio is about the same as the intensity ratio, but because the $H^{12}CN$ line has an opacity of greater than ~ 2.3, the true abundance

ratio is less than ~ 0.3, which lies well within the range of ratios measured in molecular clouds (Goldsmith *et al.* 1981). HNC, like HCN (Deguchi, Claussen, and Goldsmith 1986), is unexpected in an oxygen-rich stellar atmosphere, so its presence in the envelope is presumably a result of chemical reactions occurring subsequent to the expulsion of the gas from the star.

As in the interstellar medium (see Langer 1985) and in C-rich envelopes (Glassgold *et al.* 1986), the most likely origin of HNC is the dissociative recombination of $HCNH^+$, which can give HCN, HNC, or CN with uncertain branching ratios. However, if ionic reactions prevail, and if HCN is itself formed predominantly from dissociative recombination of $HCNH^+$, the ratio HNC/HCN should directly reflect the corresponding branching ratio. Even if HCN is formed somehow in the interior of the envelope, and HNC is not, ionic reactions such as

$$HCO^+ + HCN \rightarrow HCNH^+ + CO\,,$$
$$H_3O^+ + HCN \rightarrow HCNH^+ + H_2O\,, \qquad (7)$$

can convert HCN into HNC in the external layers. The rates of these ionic reactions with the strongly polar molecule HCN should be very large at low temperature ($\sim 10^{-8}$ cm^3 s^{-1} for HCO^+ at 100 K, Glassgold *et al.* 1986). Given the HCO^+ abundance of Table 2, we thus expect that about 10% of HCN reacts with HCO^+. However, if HCO^+ is confined to the high-velocity flow, the real abundance of HCO^+ can be larger, and that of H_3O^+ can be at least comparable according to the model of Mamon, Glassgold, and Omont (1986).

To summarize, the large abundance of HNC supports its formation by ionic chemistry. The ratio HCN/HNC either reflects the branching ratios of the dissociative recombination of $HCNH^+$, or, if there is another route for the formation of HCN and if the reshuffling of abundances by reactions with HCO^+ and H_3O^+ is incomplete, the observed ratio is an upper limit to the branching ratio.

The limit on the CN abundance is compatible with the prediction that the branching ratio for the dissociative recombination of $HCNH^+$ to produce CN and HCN + HNC is about unity (Herbst 1978). However, the branching ratio could be much smaller than unity. We expect that the CN photoproduced from HCN and HNC does not contribute significantly since, for example, in IRC +10216 where the CN is apparently photoproduced (Huggins, Glassgold, and Morris 1984), the area of the $1_{3/2} \rightarrow 0_{1/2}$ line of ^{13}CN is approximately 30 times less than that of $H^{13}CN(1\text{–}0)$ (Truong-Bach *et al.* 1987). In OH 231.8 one might expect a similar ratio for the antenna temperatures of HCN and CN if the latter was only produced by photodissociation of HCN.

e) SiO

The thermal SiO spectrum, although somewhat noisy (Fig. 1), clearly shows the predominance of the broad component toward the blue; on the red side it is absent. The narrow component is also present, although it is relatively weak. The profile area between -10 and $+70$ km s^{-1} is therefore heavily contaminated with emission in the broad component, and the abundance given in Table 2 for the region responsible for the narrow component is overestimated. As in most circumstellar envelopes where SiO is detected, the abundance of this molecule in OH 231.8 is a small fraction (in this case, $\sim 10^{-3}$) of the cosmic abundance of silicon. As SiO is the dominant carrier of Si in a cool, oxygen-rich stellar atmosphere (e.g., Tsuji 1973), the low abundance of this molecule in the envelope can be interpreted to imply that most of the silicon has been incorporated into grains (Morris *et al.* 1979). Indeed, OH 231.8 has an exceptionally deep 10 μm silicate absorption feature (Gillett and Soifer 1976). The dust-loss rate suggested by Sopka *et al.* (1984)—$2 \times 10^{-6}\,M_\odot$ yr^{-1}—is more than enough to account for all of the silicon if silicates dominate the grain content.

The small quantity of SiO detected is still far larger than predicted for this envelope by Jura and Morris (1985). Because the OH 231.8 envelope is so cold, and because it contains such a high density of dust, these authors predicted that the condensation of SiO onto grains would be essentially complete. The predominance of the broad component in the SiO profile provides three possible answers to this potential embarrassment: (1) the high-velocity shocks to which the high-latitude outflow is subjected (CDST) are sufficient to sputter material off of grains, including, presumably, SiO. (2) The streaming velocity of the dust through the gas in the high-velocity flow may be quite large. If the grains are distributed over a range of sizes, they will have a consequent distribution of streaming velocities. Under these circumstances, relatively high-velocity grain-grain collisions can occur, and SiO may be released from the grains in this fashion. (3) Indeed, if the streaming velocity exceeds about 4 km s^{-1}, the condensation of SiO onto grains will have been inhibited in the first place, because the relative kinetic energy of SiO molecules will exceed the binding energy onto grains. These three effects may also play some lesser role in the lower velocity portion of the outflow from which the narrow component of the profile arises. Some explanation like these is needed to account for why there is any SiO present at all. These hypotheses predict that the SiO abundance should vary inversely with velocity, and thus directly with latitude, provided that it is not photodissociated.

Our upper limit to the SiS abundance relates to the status of silicon. Although SiS is not expected to be present in appreciable abundances in an oxygen-rich stellar atmosphere, it might form in the outflow if free silicon were available (there is little question that the sulfur is available—see § VI below). At present, the limit to [SiS] is only about a factor of 2 below the measured CS abundance; an improved limit would help constrain the silicon chemistry.

V. THE HCO^+ CHEMISTRY

Judging from its broad, featureless profile, HCO^+ is enhanced, and possibly confined, in the high-velocity outflow at high latitudes. Thus it is mainly coincident with a region in which the UV radiation is possibly enhanced. In O-rich envelopes, HCO^+ can be produced by the reactions

$$C^+ + H_2O \rightarrow HCO^+ + H\,,$$
$$C^+ + OH \rightarrow H + CO^+(+H_2) \rightarrow HCO^+\,. \qquad (8)$$

In a model assuming galactic UV radiation alone, Mamon, Glassgold, and Omont (1986) find that these reactions lead to an amount of HCO^+ comparable to, but slightly smaller than, the one we have measured. Thus it is likely that a moderate increase of the production of C^+ could easily account for the observed HCO^+ (the abundance of HCO^+ is relatively insensitive to that of H_2O because HCO^+ is both formed and destroyed by reactions with H_2O).

Other molecular ions—N_2H^+ and HCS^+—were also sought in OH 231.8, the first because CDST have claimed that the envelope is nitrogen-rich, and the second because of the

broad array of other sulfur-containing molecules that are seen, and because of the chemical analogy with HCO^+. Neither was detected. The abundance limit for N_2H^+—about $\frac{1}{5}$ of the observed HCO^+ abundance—is consistent with the expectation that it has a smaller production rate than HCO^+, and that H_3^+ is not the major source of HCO^+ here. The most likely source of N_2H^+ is H_3^+ produced by cosmic rays (Glassgold, Lucas, and Omont 1986; Glassgold *et al.* 1987). Then because of the fast destruction of N_2H^+ by H_2O and CO, even with a large overabundance of N_2, the expected abundance of N_2H^+ is almost an order of magnitude smaller than our upper limit.

VI. SULFUR

One of the most noteworthy characteristics of the OH 231.8 spectrum is the multitude of lines from sulfur-containing molecules, including SO_2, SO, H_2S, CS, and OCS. The implied abundances of these molecules is relatively high, especially that of SO_2. The total abundance of sulfur molecules, by number relative to H_2, is 1.7×10^{-5} ($10^{-4}\ M_\odot\ \mathrm{yr}^{-1}/\dot{M}$), which is large enough to place an important constraint on the total mass-loss rate. If standard cosmic abundances apply to this object (a supposition which has been questioned by Jura and Morris [1985] and which is not completely consistent with the data of CDST), then, since $([S]/[H])_{\mathrm{cosmic}} = 1.6 \times 10^{-5}$, the mass-loss rate must exceed $5 \times 10^{-5}\ M_\odot\ \mathrm{yr}^{-1}$. If any of the lines are optically thick, as may well be the case for SO_2, the total sulfur abundance, and thus the minimum mass-loss rate, must be even larger. This result is consistent with the mass-loss rate determined by others (Soifer *et al.* 1981; Morris, Bowers, and Turner 1982; Knapp and Morris 1985), all using different methods, but all implicitly assuming cosmic abundances.

For sulfur, however, deviations from cosmic abundances are not likely to affect the implied minimum mass-loss rate. The star (or stars) in the system is probably not much more massive than about $3\ M_\odot$, the turnoff mass of the open cluster M46, in which OH 231.8 apparently lies (Jura and Morris 1985). Therefore, normal nuclear processing in this system cannot proceed past helium-burning, and the relative mass of sulfur will not be affected. The deviations from cosmic abundances that are indicated—enhanced N and probably enhanced $[^{13}C]/[^{12}C]$—can be accounted for by CNO-processing.

It is not entirely excluded that sulfur is enhanced in some way. If this system has undergone a nova episode in the past (Jura and Morris 1985), and has somehow retained the nucleosynthetic products of the nova, sulfur is very likely to be enhanced in the circumstellar material according to the observational (Snijders *et al.* 1984) and theoretical (Hillebrandt 1986) evidence on novae. A measurement of sulfur isotope ratios would provide a useful discriminant for assessing this possibility, since the relative production rate of the rarer sulfur isotopes in novae is predicted to be considerably less than their relative cosmic abundances (Hillebrandt 1986). We also note that a sulfur overabundance has been reported for the low-mass, Population II star HD 46703 by Bond and Luck (1987), who speculate that "Excess ^{32}S might be synthesized during a high-temperature episode in the core (possibly the core helium flash) through successive alpha captures on ^{12}C." Again, the sulfur isotope ratios would be a useful discriminant.

Barring an anomalous sulfur production mechanism, however, we conclude that the data on sulfur molecules provide the strongest evidence that the mass-loss rate of OH 231.8 is $\sim 10^{-4}\ M_\odot\ \mathrm{yr}^{-1}$. The use of this mass-loss rate to scale the abundances reported in Table 2 is therefore appropriate, at least if the values of f are rescaled to represent mass fractions.

An important common characteristic of the profiles of all the sulfur-containing molecules is the absence of the broad emission component. This is especially noteworthy for the SO_2 profile, which has a large signal-to-noise ratio. We infer from this that sulfur chemistry is not active at the high latitudes (although the sulfur is not lacking: CDST report relatively strong [S II] line emission from the HH knots lying along the polar axis), possibly because the environment is too hostile.

The observations that SO_2 is the dominant sulfur species in the external envelope is foreseen by the model of Scalo and Slavsky (1980) and Slavsky and Scalo (1986). However, if a larger, more realistic photodissociation rate of SO_2 is adopted, thus enhancing S^+ production, it is difficult to explain the large SO_2 abundance in OH 231.8+4.2 (Guilloteau *et al.* 1986). As for NH_3 the relatively large abundance observed for H_2S implies that the abundance of H is very small, since the reaction

$$H_2S + H \rightarrow HS + H_2 \qquad (9)$$

proceeds rather quickly. A possible formation route for CS could be the equivalent of reaction (5):

$$H_2S + C^+ \rightarrow HCS^+ + H\ . \qquad (10)$$

VII. SUMMARY

The OH 231.8 system provides us with an unusual opportunity to acquire information on two subjects: circumstellar chemistry and stellar evolution. Until recently, the study of chemistry in oxygen-rich circumstellar envelopes was confined predominantly to the theoretical domain because of the paucity of observed nonmaser molecular lines. With the rich molecular line spectrum of OH 231.8, we now have an environment which can be used to assess the chemical models. However, because internal ionization appears to play a significant role in the chemistry of OH 231.8 and because high-velocity shocks appear to be present, it is not a typical circumstellar environment. These phenomena promote the chains of reactions leading to the observed variety of molecules. In more common types of oxygen-rich circumstellar envelopes, such as OH/IR stars, the ionization is expected to be predominantly external (Mamon, Glassgold, and Omont 1986), and the shocks that may be present are weaker. Therefore, the reaction chains are initiated less frequently, with the result that the relative abundances in these envelopes of many of the species observed in OH 231.8 are much smaller than in OH 231.8 itself. A notable exception may be OH 26.5 (Guilloteau *et al.* 1986), which is also an extreme object.

The axisymmetric outflow of OH 231.8 stems from a star (or stars) in a crucial, short phase of its evolution. The large extent of the outflowing envelope should permit one (using radio interferometry) to literally read the recent history of this system by studying the radial and angular distributions of composition and velocity. The most important outstanding problem in this system is understanding the cause of the bipolarity. If further work can verify that OH 231.8 is a binary system containing an accretion disk, we stand to learn a great deal about the properties of the accretion disk.

We are grateful to B. Reipurth for communicating data prior to publication, and we thank M. Jura and Ben Zuckerman for

helpful comments on the manuscript. This work has been partially supported by NSF grants 83-18342 and 84-13862 to UCLA, and by the ATP "Molecules Interstellaires" of CNRS. The 100 m telescope is operated by the Max-Planck-Institut für Radioastronomie, Bonn, Federal Republic of Germany. M. M. acknowledges the hospitality of the Groupe d'Astrophysique of the Observatoire de Grenoble, where part of this work was carried out.

REFERENCES

Allen, D. A., Barton, J. R., Gillingham, P. R., and Phillips, B. A. 1980, *M.N.R.A.S.*, **190**, 531.
Barvainis, R., and Clemens, D. P. 1984, *A.J.*, **89**, 1833.
Betz, A. L., and McLaren, R. A. 1980, in *Interstellar Molecules, IAU Symposium 87*, ed. B. H. Andrew (Dordrecht: Reidel), p. 503.
Bond, H. E., and Luck, R. E. 1987, *Ap. J.*, **312**, 203.
Bowers, P. F., and Morris, M. 1984, *A.J.*, **276**, 646.
Cohen, M. 1981, *Pub. Astr. Soc. Pacific*, **93**, 288.
———. 1985, in *Mass Loss from Red Giants*, ed. M. Morris and B. Zuckerman (Dordrecht: Reidel), p. 274.
Cohen, M., Dopita, M. A., Schwartz, R. D., and Tielens, A. G. G. M. 1985, *A.J.*, **297**, 702 (CDST).
Deguchi, S., Claussen, M. J., and Goldsmith, P. F. 1986, *A. J.*, **303**, 810.
Deguchi, S., and Goldsmith, P. 1985, *Nature*, **317**, 336.
Dyck, H. M., Zuckerman, B., Leinert, Ch., and Beckwith, S. 1984, *Ap. J.*, **287**, 801.
Feast, M. W., Catchpole, R. M., Whitelock, P. A., Roberts, G., Spencer Jones, J., and Carter, B. S. 1983, *M.N.R.A.S.*, **203**, 1207.
Gillett, F. C., and Soifer, B. T. 1976, *A.J.*, **207**, 780.
Glassgold, A. E., Lucas, R., and Omont, A. 1986, *Astr. Ap.*, **157**, 35.
Glassgold, A. E., Mamon, G., Omont, A., and Lucas, R. 1987, *Astr. Ap.*, submitted.
Goldsmith, P. F., Langer, W. D., Ellder, J., Irvine, W., and Kollberg, E. 1981, *Ap. J.*, **249**, 524.
Guilloteau, S., Lucas, R., Rieu, N.-Q., and Omont, A. 1986, *Astr. Ap.*, **165**, L1.
Herbst, E. 1978, *A.J.*, **222**, 508.
Hillebrandt, W. 1986, in *Advances in Nuclear Astrophysics*, ed. E. Vangioni-Flam, *et al.* (Gif-sur-Yvette: Ed. Frontieres).
Hollenbach, D., and McKee, C. F. 1980, *Ap. J. (Letters)*, **241**, L47.
Huggins, P. J., Glassgold, A. E., and Morris, M. 1984, *A.J.*, **279**, 284.
Johansson, L. E. B., *et al.* 1984, *Astr. Ap.*, **130**, 227.
Jura, M., and Morris, M. 1985, *A.J.*, **292**, 487.
Kleinmann, S. G., Sargent, D. G., Moseley, H., Harper, D. A., Loewenstein, R. F., Telesco, C. M., and Thronson, H. A., Jr. 1978, *Astr. Ap.*, **65**, 139.
Knapp, G. R., and Chang, K. M. 1985, *A.J.*, **293**, 281.
Knapp, G. R., and Morris, M. 1985, *A.J.*, **292**, 640.
Langer, W. 1985, in *Birth and Infancy of Stars, Les Houches XLI*, ed. R. Lucas, A. Omont, and R. Stora (Amsterdam: North Holland), p. 279.
Mamon, G., Glassgold, A. E., and Omont, A. 1987, *Ap. J.*, in press.
Mitchell, G. F. 1984, *Ap. J. Suppl.*, **54**, 81.
Morris, M. 1981, *Ap. J.*, **249**, 572.
———. 1985, in *Mass Loss from Red Giants*, ed. M. Morris and B. Zuckerman (Dordrecht: Reidel), p. 124.
Morris, M., and Bowers, P. F. 1980, *A.J.*, **85**, 724.
Morris, M., Bowers, B., and Turner, B. E. 1982, *A.J.*, **259**, 625.
Morris, M., and Knapp, G. R. 1976, *A.J.*, **204**, 415.
Morris, M., Lucas, R., and Omont, A. 1985, *Astr. Ap.*, **142**, 147.
Morris, M., Redman, R., Reid, M. J., and Dickinson, D. F. 1979, *Ap. J.*, **229**, 257.
Olofsson, H., Johansson, L. E. B., Hjalmarson, A., and Nguyen-Quang-Rieu 1982, *Astr. Ap.*, **107**, 128.
Reipurth, B. 1987, *Nature*, **325**, 787.
Scalo, J. M., and Slavsky, D. B. 1980, *Ap. J. (Letters)*, **293**, L73.
Slavsky, D. B., and Scalo, J. M. 1986, preprint.
Snijders, M. A. J., Batt, T. J., Seaton, M. J., Blades, J. C., and Morton, D. C. 1984, *M.N.R.A.S.*, **211**, 7P.
Soifer, B. T., Willner, S. P., Capps, R. W., and Rudy, R. J. 1981, *Ap. J.*, **250**, 631.
Sopka, R. J., Hildebrand, R., Jaffe, D. T., Gatley, I., Roellig, T., Werner, M., Jura, M., and Zuckerman, B. 1985, *Ap. J.*, **294**, 242.
Tielens, A. G. G. M., Werner, M., and Capps, R. 1985, in *Mass Loss from Red Giants*, ed. M. Morris and B. Zuckerman (Dordrecht: Reidel), p. 287.
Truong-Bach, T., Nguyen-Q-Rieu, Omont, A., Olofsson, H., and Johansson, L. E. B. 1987, *Astr. Ap.*, in press.
Tsuji, T. 1964, *Ann. Tokyo Astron. Obs.*, 2nd ser. **9**, 1.
———. 1973, *Astr. Ap.*, **23**, 411.
Turner, B. E. 1971, *Ap. Letters*, **8**, 73.
Ukita, N., and Morris, M. 1983, *Astr. Ap.*, **121**, 15.

STÉPHANE GUILLOTEAU, ROBERT LUCAS, and ALAIN OMONT: Groupe d'Astrophysique, Observatoire de Grenoble, Université Scientifique Technologique et Médicale de Grenoble, CERMO B.P. 68, 38402 St. Martin d'Hères Cedex, France

MARK MORRIS: Department of Astronomy, Math-Sciences Bldg., UCLA, Los Angeles, CA 90024